Supplementary Information

Cryo-EM structure-based selection of computed ligand poses enables design of MTA-synergic PRMT5 inhibitors of better potency

Wei Zhou[1,2,&‡], Gaya P. Yadav[3,4,&‡], Xiaozhi Yang[1,2], Feng Qin[5], Chenglong Li[1,2,6,*], and Qiu-Xing Jiang[1,3,4,5,*#]

1. Department of Medicinal Chemistry, College of Pharmacy, University of Florida, Gainesville, FL 32610, United States.

2. Department of Biochemistry and Molecular Biology, College of Medicine, University of Florida, Gainesville, FL 32610, United States.

3. Department of Microbiology and Cell Science, University of Florida, 1355 Museum Drive, Gainesville, FL 32611, United States

4. Laboratory of Molecular Physiology and Biophysics, Hauptmann-Woodward Medical Research Institute, Buffalo, NY 14203, United States.

5. Department of Physiology and Biophysics, University at Buffalo, Buffalo 14214, United States.

6. Center for Natural Products, Drug Discovery and Development (CNPD3), University of Florida, Gainesville, FL 32610, United States.

& Current addresses: (G.P.Y.): Department of Biochemistry and Biophysics, Texas A &M University, College Station, TX 77843, United States.

List of supplementary items:

Supplementary Figures 1-9

Supplementary Tables 1-7

Supplementary References

Supplementary Figures and legends:

Supplementary Figure 1. PRMT5:MEP50 complex purification and characterization.

a). Size exclusion chromatography of the PRMT5:MEP50 complex after anti-FLAG affinity column. Fractions at the indicated area were collected and concentrated. **b).** An SDS-PAGE gel is shown for the collected fractions of PRMT5:MEP50 with a purity greater than 95%. **c).** Sedimentation velocity analytical ultracentrifugation (SV-AUC). The PRMT5:MEP50 complex has an estimated mass of 445 kDa.

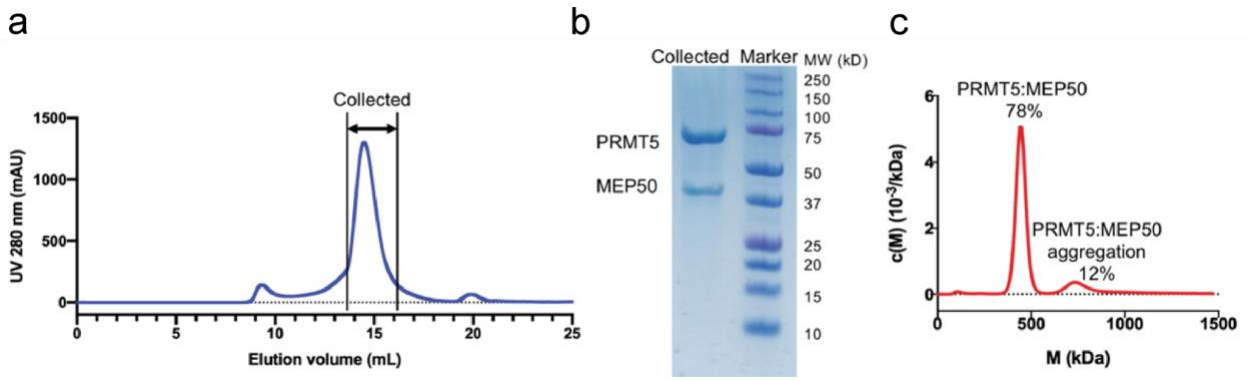

Supplementary Figure 2. Processing cryo-EM data of the PRMT5: MEP50/ 11-2F/ MTA complex. The final map has an overall nominal resolution of 3.14 Å (FSC=0.143). The presentations were prepared in Chimera [1] and PyMOL[2].

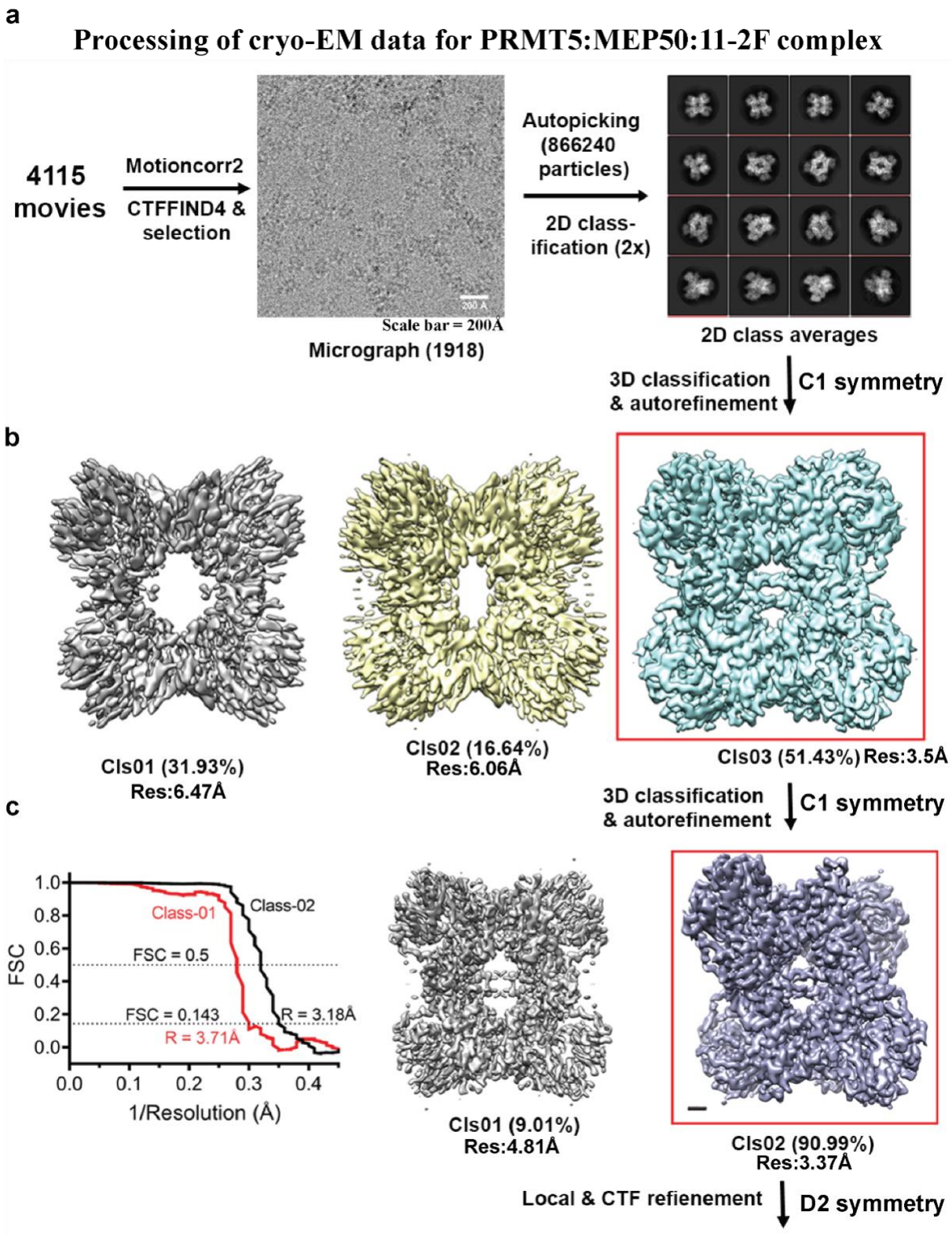

d

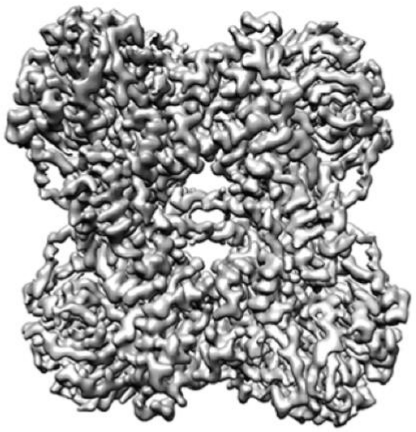

Final map (207392 particles)
(Res = 3.14Å, D2 symmetry)

e

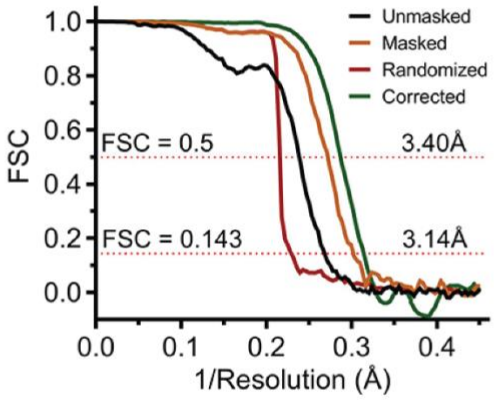

FSC curve

f

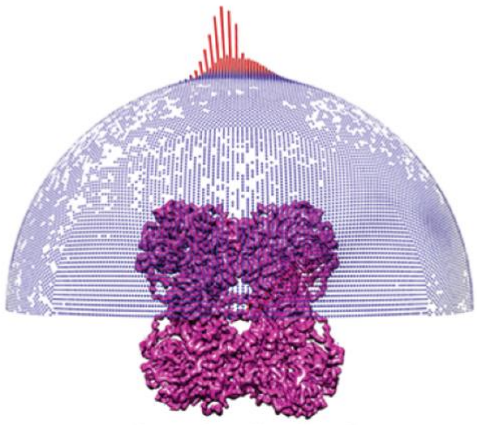

Angular distribution

Supplementary Figure 3. Top poses of different ligands from computational analysis
a). Top 8 poses of MTA. In each of the 2,000 runs, 25 million seed positions were used as starting points for movements and energy minimization. The top poses from 2,000 runs were clustered based on their RMSD. The best ones of the resultant 8 clusters are showed.

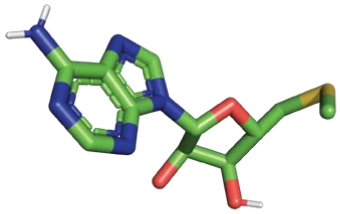

Cluster 1

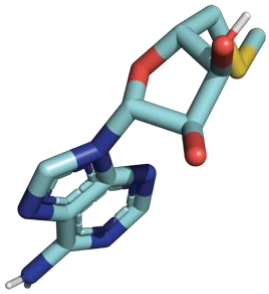

Cluster 2

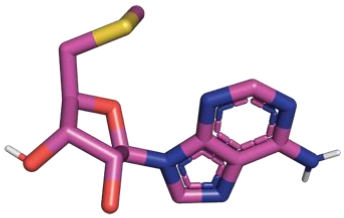

Cluster 3

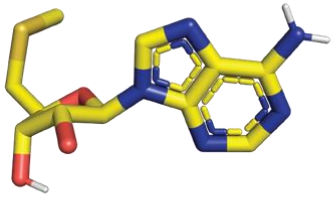

Cluster 4

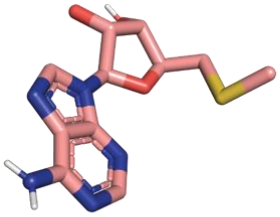

Cluster 5

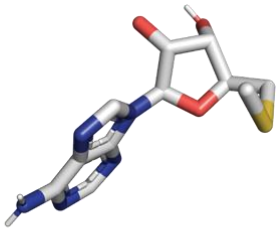

Cluster 6

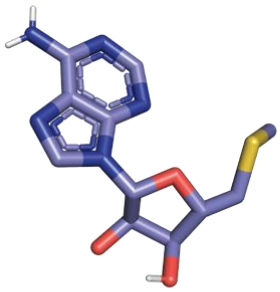

Cluster 7

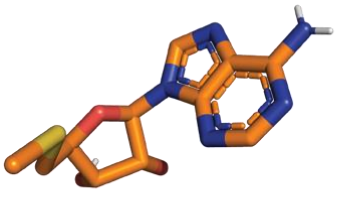

Cluster 8

b). Top 10 poses of SAH came from analysis as explained in a.

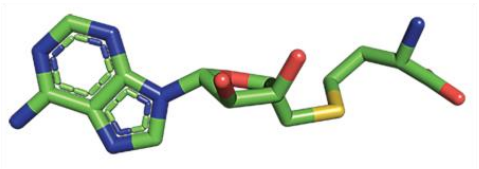

Cluster 1

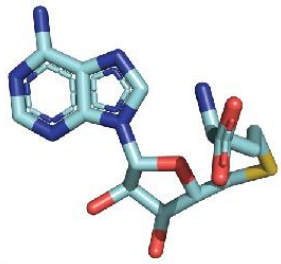

Cluster 2

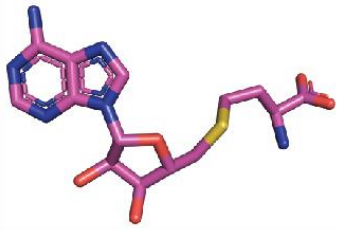

Cluster 3

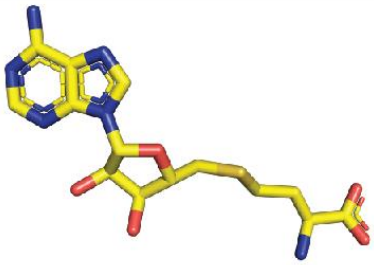

Cluster 4

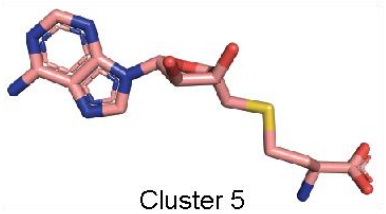

Cluster 5

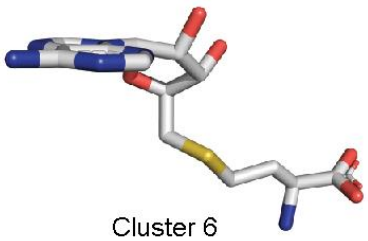

Cluster 6

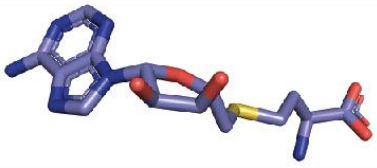

Cluster 7

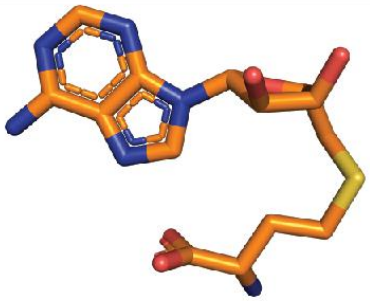

Cluster 8

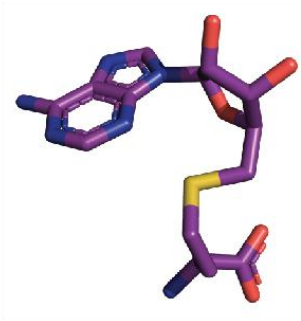

Cluster 9

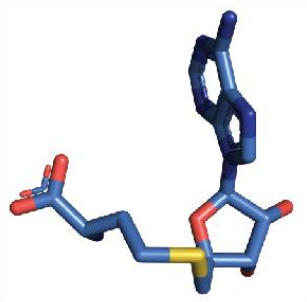

Cluster 10

c). Top 10 poses of SAM.

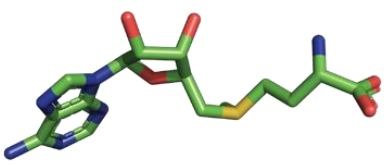

Cluster 1

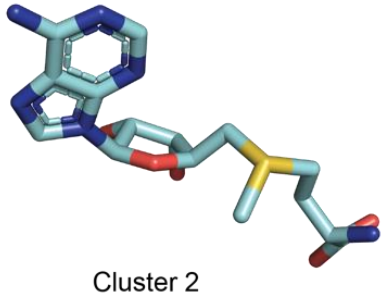

Cluster 2

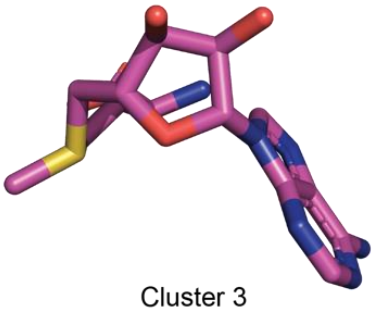

Cluster 3

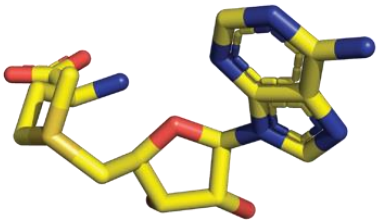

Cluster 4

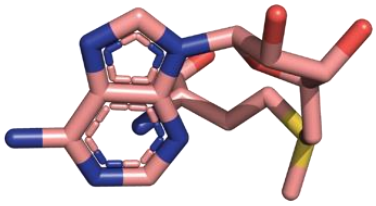

Cluster 5

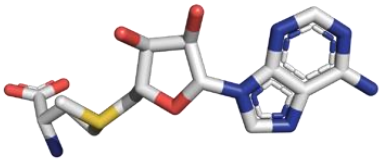

Cluster 6

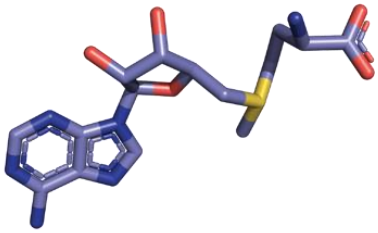

Cluster 7

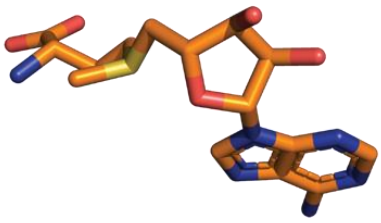

Cluster 8

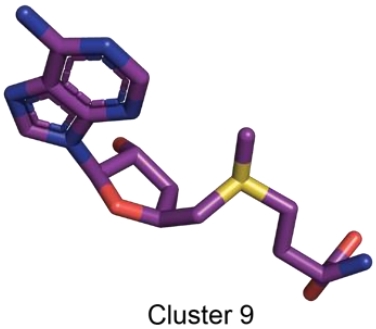

Cluster 9

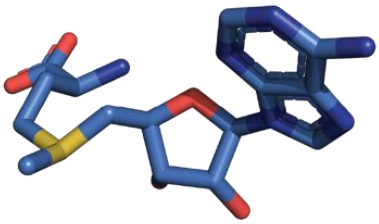

Cluster 10

d). Top 10 poses of 11-2F.

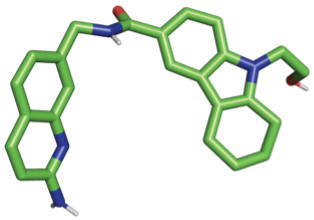

Cluster 1

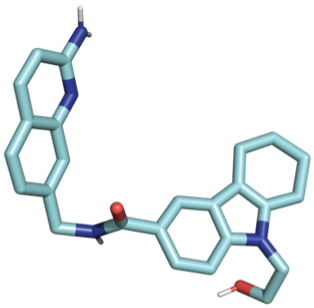

Cluster 2

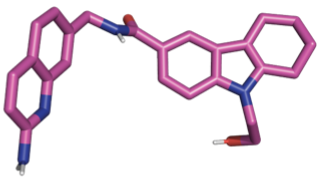

Cluster 3

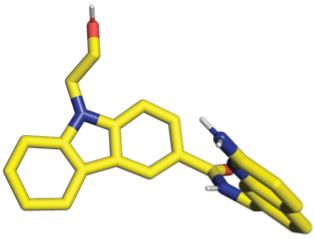

Cluster 4

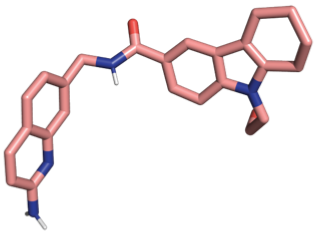

Cluster 5

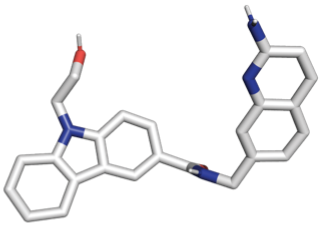

Cluster 6

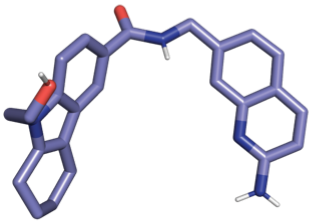

Cluster 7

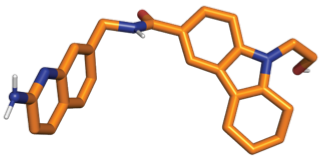

Cluster 8

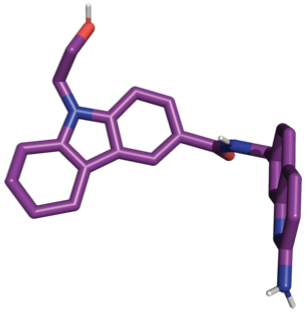

Cluster 9

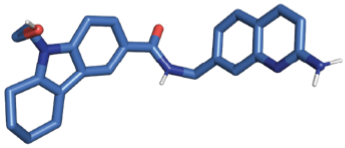

Cluster 10

e). Two opposite orientations of 11-2F differ in docking energy. The refined pose in yellow and the other pose representing cluster 4 (white) are fitted into the cryo-EM density map of the ligand (semitransparent grey). The two had their head and tail parts in opposite arrangements and were not distinguished reliably by fitting ligand atoms into the cryo-EM density at the current 3.1 Å resolution.

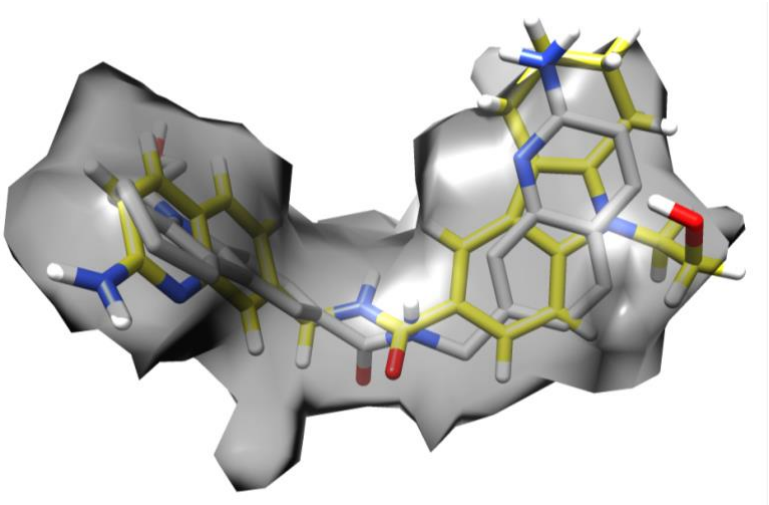

f). Two opposite orientations of 11-2F inside the binding pocket. The residues in the binding pocket (blue mesh) did not change significantly to accommodate the two poses. The refinement statistics in PHENIX for PRMT5 and ligands with 11-2F in two opposite orientations in the binding pocket (cyan vs. pink) were the same as in Table 1.

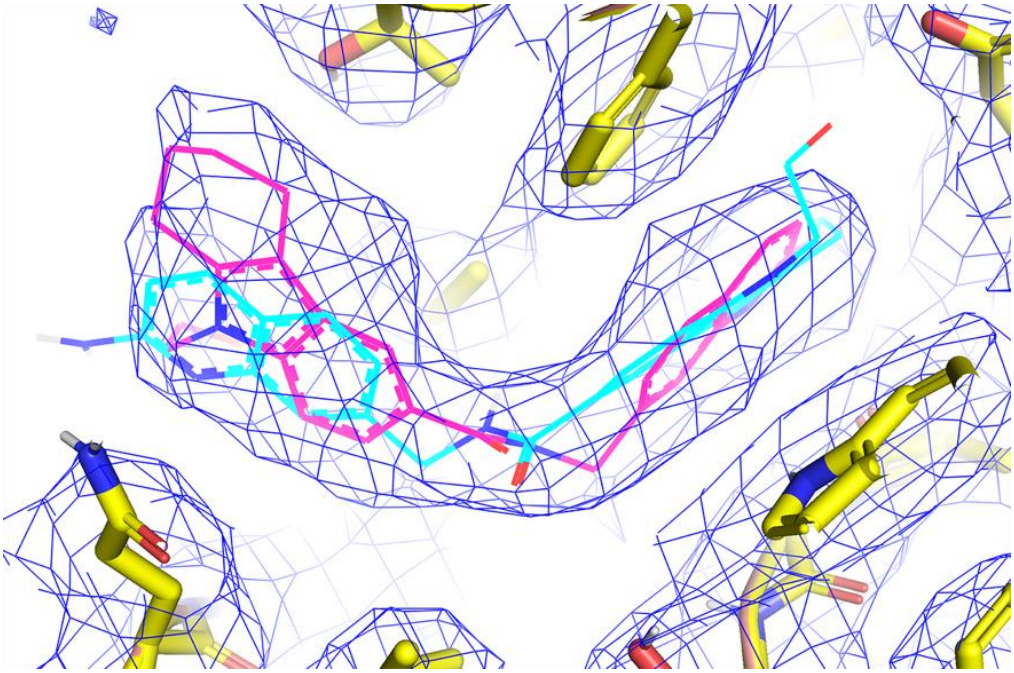

Supplementary Figure 4. Processing cryo-EM data of the *apo* PRMT5: MEP50 complex. The final map is of 3.2 Å (FSC = 0. 143). Presentations were prepared in Chimera [1] and PyMOL [2].

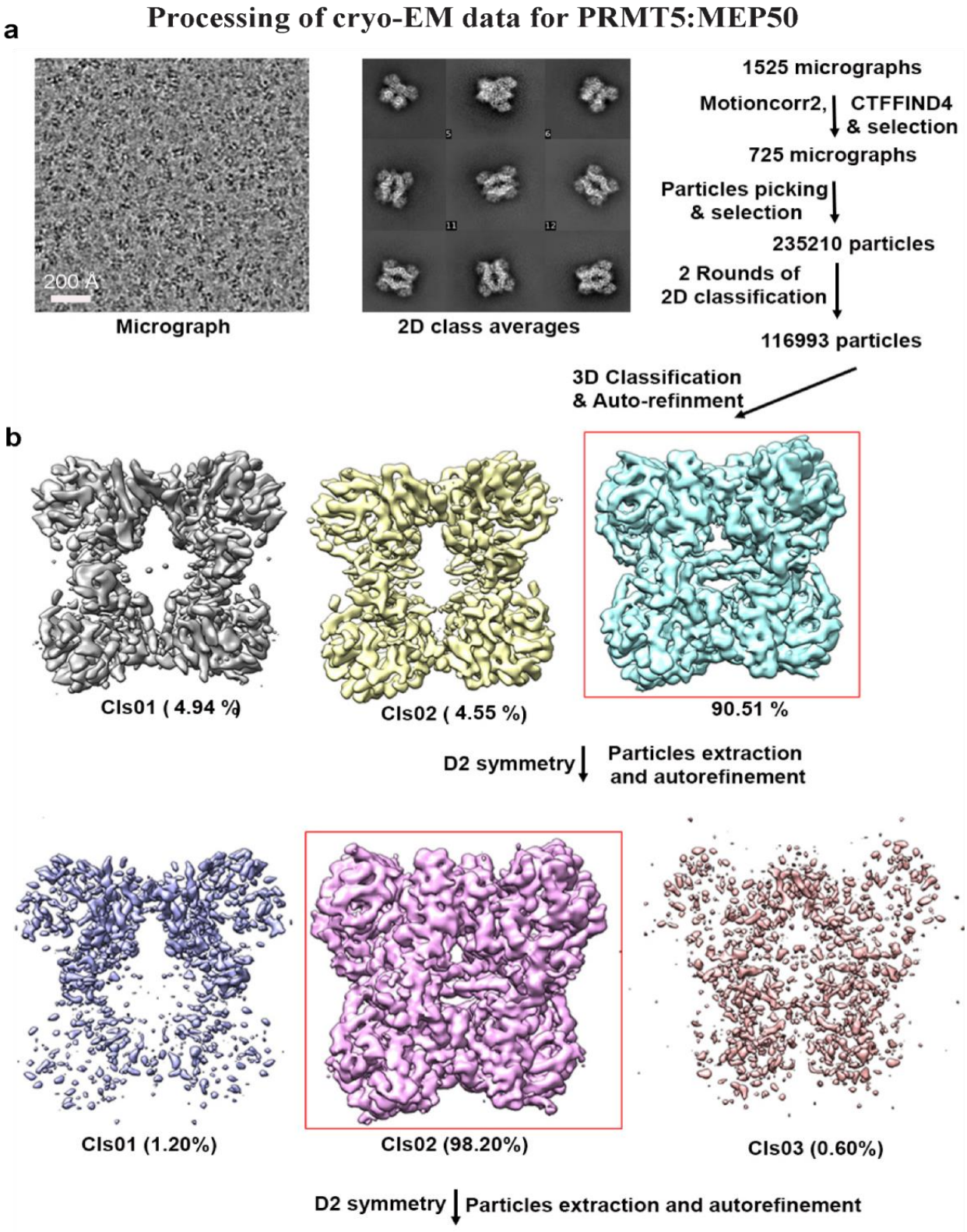

C

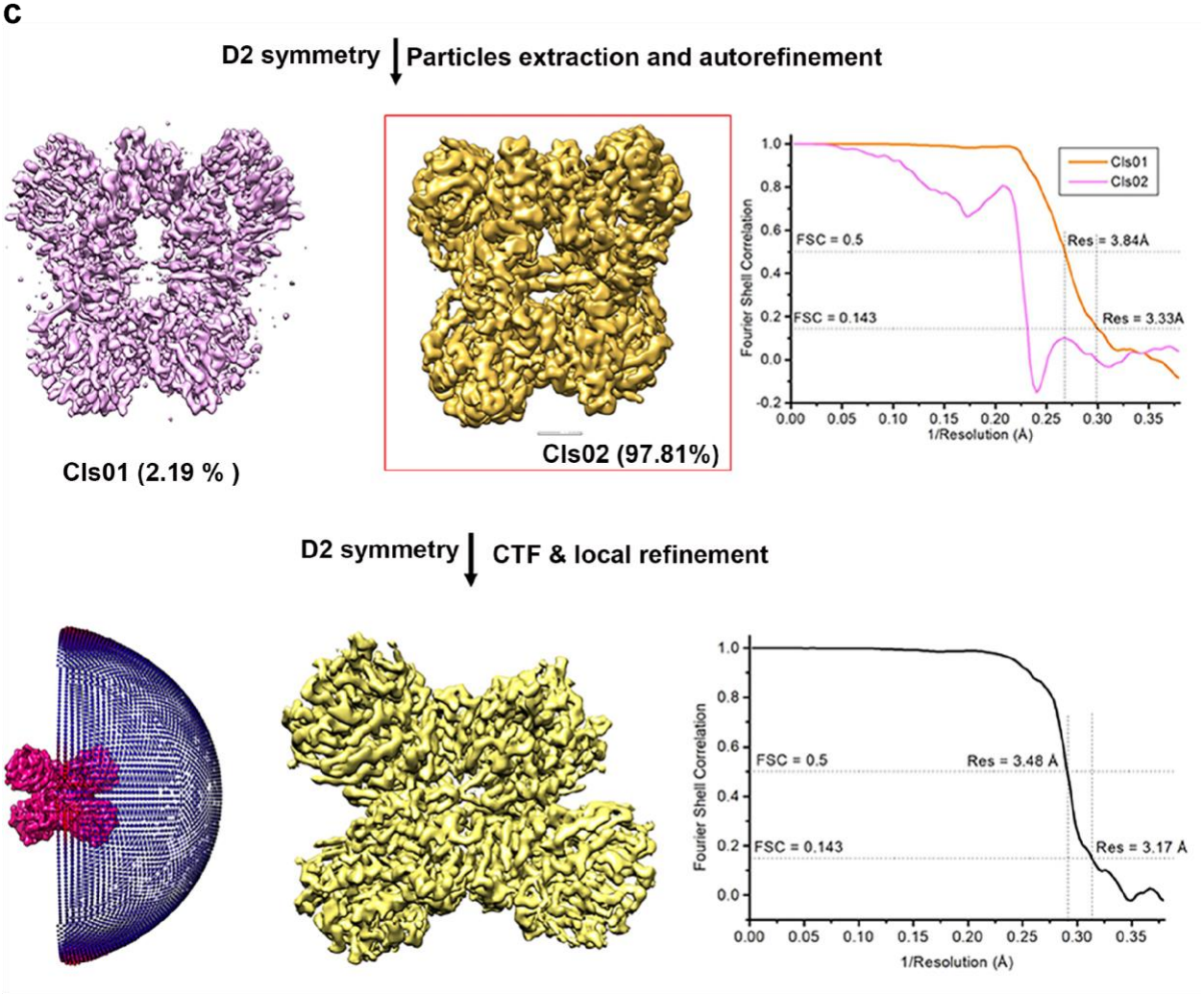
D2 symmetry
Particles extraction and autorefinement
Cls01 (2.19 %)
Cls02 (97.81%)
Cls01
Cls02
FSC = 0.5
Res = 3.84Å
FSC = 0.143
Res = 3.33Å
Fourier Shell Correlation
1/Resolution (Å)
D2 symmetry
CTF & local refinement
FSC = 0.5
Res = 3.48 Å
FSC = 0.143
Res = 3.17 Å
Fourier Shell Correlation
1/Resolution (Å)

Supplementary Figure 5. Sequence alignment of PRMT1 - 7 focusing on their catalytic domains. Key residues conserved among the catalytic domains are highlighted (*, :).

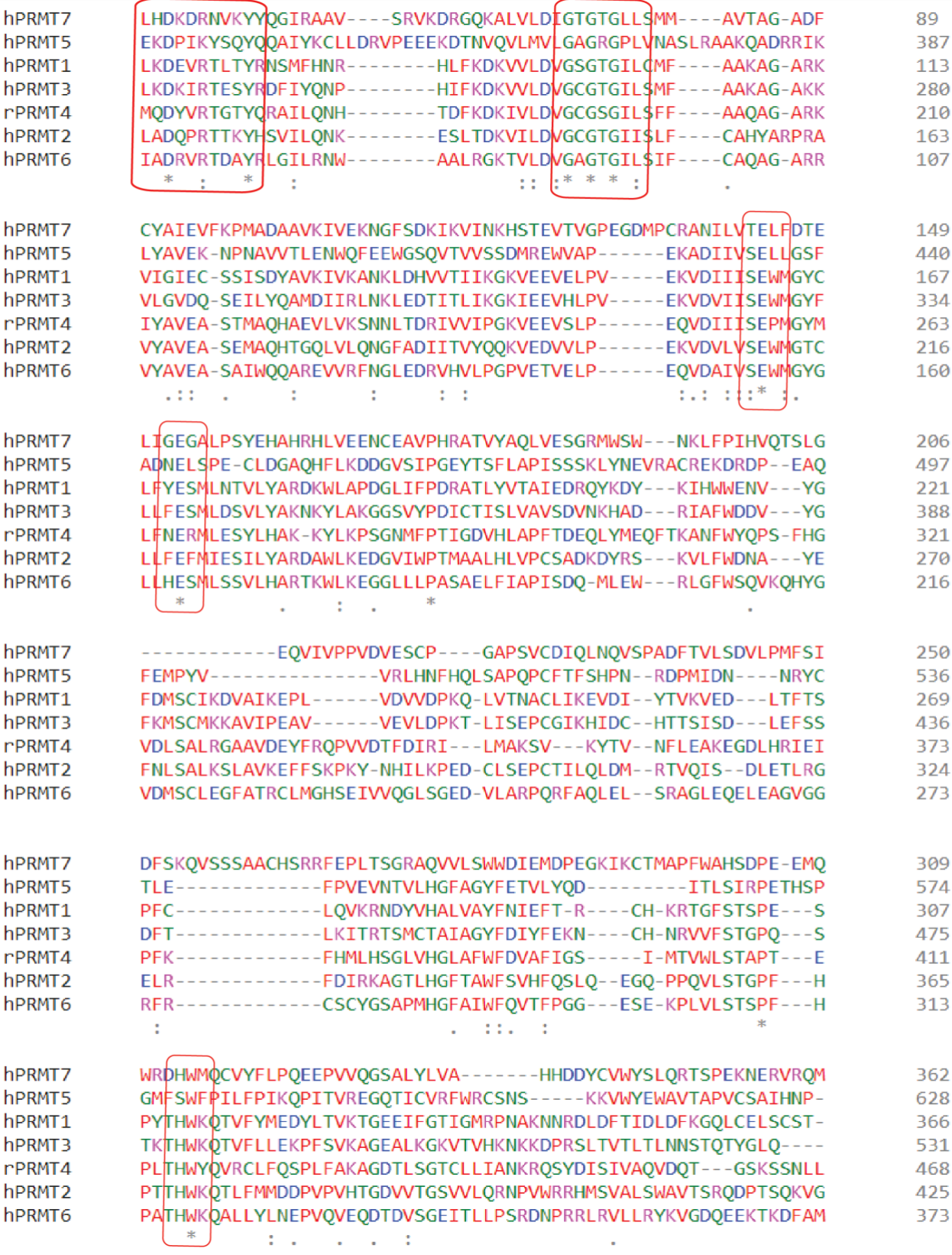

Supplementary Figure 6. Top 10 poses of 11-9F from computational analysis.

Cluster 1

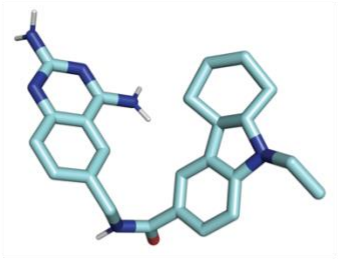

Cluster 2

Cluster 3

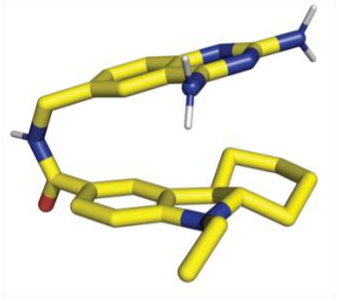

Cluster 4

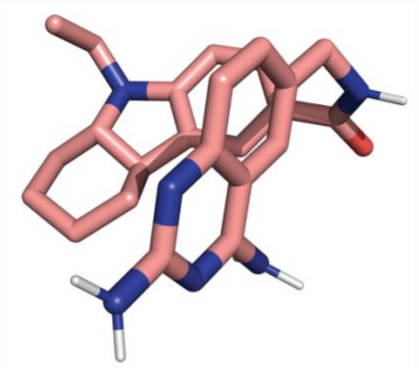

Cluster 5

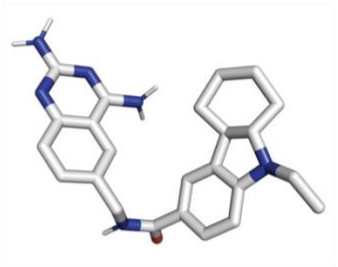

Cluster 6

Cluster 7

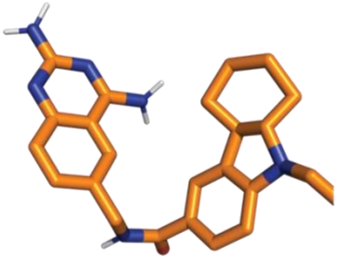

Cluster 8

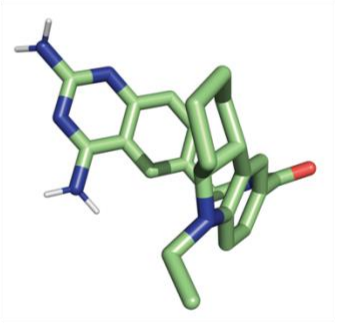

Cluster 9

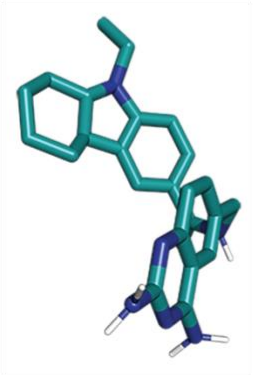

Cluster 10

Supplementary Figure 7. Top 10 poses of HWIem2104 from computational analysis.

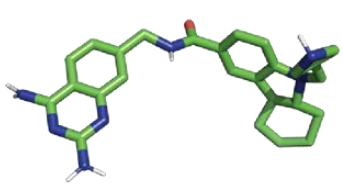

Cluster 1

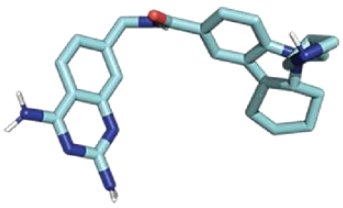

Cluster 2

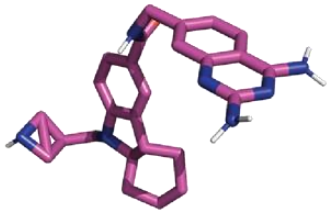

Cluster 3

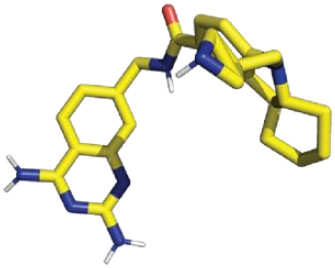

Cluster 4

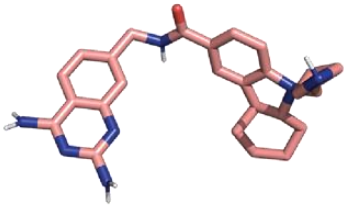

Cluster 5

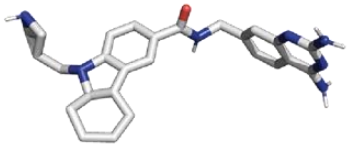

Cluster 6

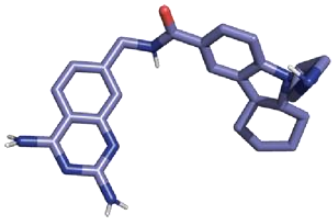

Cluster 7

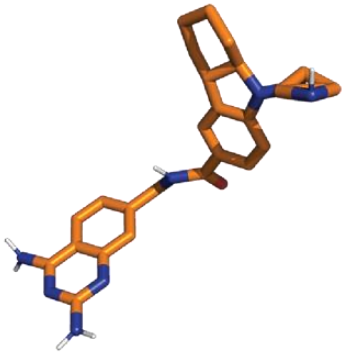

Cluster 8

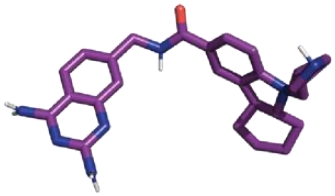

Cluster 9

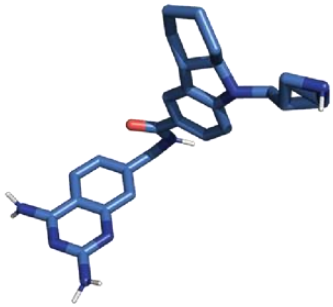

Cluster 10

Supplementary Figure 8. Top 10 poses of HWIem2109 from computational analysis.

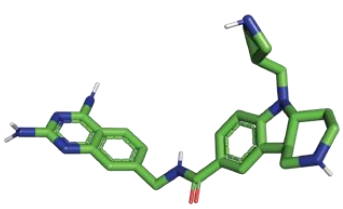

Cluster 1

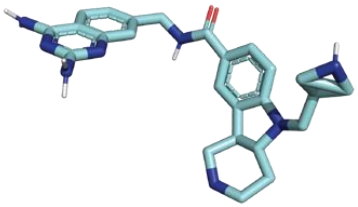

Cluster 2

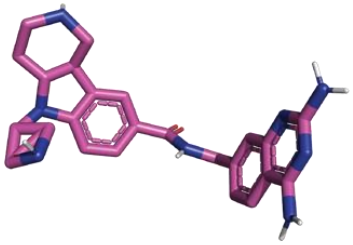

Cluster 3

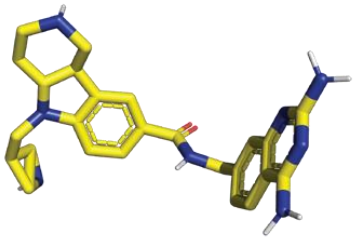

Cluster 4

Cluster 5

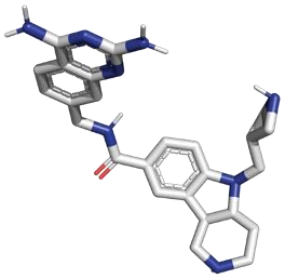

Cluster 6

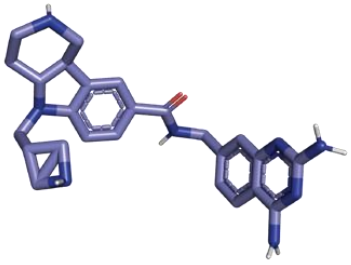

Cluster 7

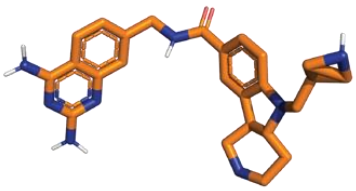

Cluster 8

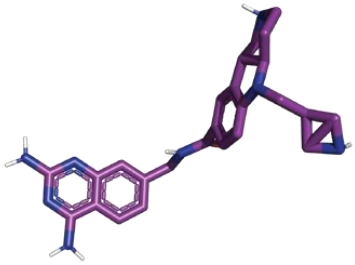

Cluster 9

Cluster 10

Supplementary Figure 9. Uncropped image from western blotting of SDMA

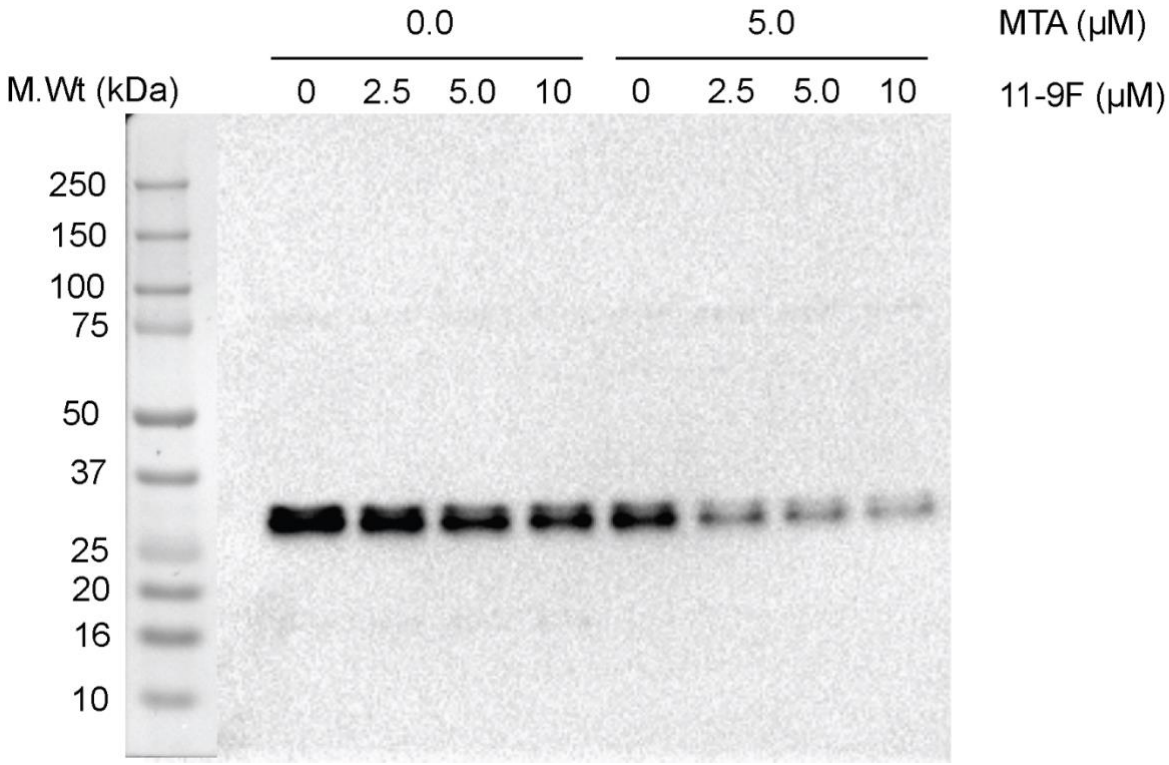

Supplementary Tables 1- 7:

Supplementary Table 1. Clusters of energy-minimized poses for MTA

Cluster Rank	Lowest Binding Energy	Run	Mean Binding Energy	Num in Clus
1	-6.63	1556	-6.03	1781
2	-5.95	241	-5.39	104
3	-5.62	1994	-5.54	48
4	-5.49	1083	-5.45	32
5	-5.21	1555	-5.17	4
6	-5.18	107	-5.18	1
7	-5.06	526	-4.94	24
8	-4.97	837	-4.97	6

Supplementary Table 2. Clusters of energy-minimized poses for SAH

Cluster Rank	Lowest Binding Energy	Run	Mean Binding Energy	Num in Clus
1	-8.80	1101	-8.13	346
2	-8.64	1726	-7.88	163
3	-8.46	9	-7.91	177
4	-8.30	694	-7.82	151
5	-8.28	496	-7.69	227
6	-7.82	353	-7.36	162
7	-7.78	1750	-7.53	24
8	-7.64	656	-7.33	15
9	-7.59	520	-6.97	241
10	-7.52	1639	-6.81	39

Supplementary Table 3. Clusters of energy-minimized poses for SAM

Cluster Rank	Lowest Binding Energy	Run	Mean Binding Energy	Num in Clus
1	-8.65	1187	-8.22	112
2	-8.55	1520	-8.26	128
3	-8.12	276	-8.15	197
4	-7.99	1993	-7.93	256
5	-7.80	1899	-7.73	373
6	-7.80	653	-7.72	3
7	-7.75	1018	-7.71	50
8	-7.38	129	-7.17	30
9	-7.27	1644	-7.53	22
10	-7.17	1824	-7.51	3

Supplementary Table 4. Clusters of energy-minimized poses for 11-2F

Cluster Rank	Lowest Binding Energy	Run	Mean Binding Energy	Num in Clus
1	-10.99	301	-10.18	49
2	-10.92	825	-10.43	70
3	-10.38	875	-9.72	10
4	-10.38	1353	-9.68	540
5	-10.36	234	-9.68	24
6	-10.21	512	-9.74	173
7	-10.13	304	-9.67	20
8	-10.10	1757	-9.28	11
9	-9.92	1551	-9.37	22
10	-9.89	217	-9.28	114

Supplementary Table 5: Clusters of energy-minimized poses for 11-9F

Cluster Rank	Lowest Binding Energy	Run	Mean Binding Energy	Num in Clus
1	-10.95	1852	-10.43	1120
2	-10.80	42	-10.47	93
3	-10.64	1780	-10.58	4
4	-10.59	1386	-10.24	3
5	-10.25	626	-9.84	20
6	-10.09	68	-9.86	10
7	-10.08	1179	-9.93	20
8	-10.07	110	-9.33	17
9	-10.03	18	-9.84	23
10	-10.02	1457	-9.88	14

Supplementary Table 6. Clusters of energy-minimized poses for HWIem2104

Cluster Rank	Lowest Binding Energy	Run	Mean Binding Energy	Num in Clus
1	-12.67	968	-11.98	1117
2	-12.64	1222	-11.54	160
3	-11.60	6	-10.62	284
4	-11.29	531	-10.17	4
5	-11.24	394	-10.75	14
6	-11.23	23	-10.57	5
7	-10.93	1715	-10.93	1
8	-10.82	446	-10.53	34
9	-10.63	1067	-10.31	15
10	-10.23	1373	-10.03	10

Supplementary Table 7. Clusters of energy-minimized poses for HWIem2109

Cluster Rank	Lowest Binding Energy	Run	Mean Binding Energy	Num in Clus
1	-12.26	725	-11.56	420
2	-11.69	879	-11.06	290
3	-10.98	1254	-10.48	911
4	-10.83	631	-10.14	44
5	-10.28	1034	-9.81	58
6	-10.27	1291	-9.72	21
7	-10.24	1561	-9.96	173
8	-10.22	169	-10.22	1
9	-10.21	939	-9.86	6
10	-10.12	754	-10.12	1

Supplementary References:

1 Pettersen, E. F. *et al.* UCSF Chimera--a visualization system for exploratory research and analysis. *J Comput Chem* **25**, 1605-1612, doi:10.1002/jcc.20084 (2004).

2 The PyMOL Molecular Graphics System. v. 2.0 (Schrodinger, LLC, 2020).